Proceedings of the
44th IEEE Conference on Decision and Control, and
the European Control Conference 2005
Seville, Spain, December 12-15, 2005

Experiments on Stabilizing Receding Horizon Control of Visual Feedback System with Planar Manipulators

Yujiro Nakaso, Yasunori Kawai and Masayuki Fujita

Abstract— **This paper deals with an application of receding horizon control to a visual feedback system. The visual feedback system consists of a planar manipulator and a camera. A terminal cost is used instead of terminal constraints on receding horizon control to guarantee the stability and to simplify the computational demand. The use of the terminal cost derived from the energy function of the visual feedback system is a key point. Then, under some conditions, the terminal cost is given as the control Lyapunov function by the inverse optimality. As an application, we apply this result to the two-link direct drive manipulator with a camera. Experimental results are compared with respect to stability and performance by applying the receding horizon control and the inverse optimal control to the planar visual feedback system. Responses of receding horizon control are compared with those of inverse optimal control and passivity based control. Furthermore, it is shown that the horizon length plays an important role for the performance.**

I. INTRODUCTION

The receding horizon control, recognized also as model predictive control, is well-known control strategy. For process control, it has been widely used nowadays. For relatively fast systems, however, few implementations of the receding horizon control have been reported recently [1]. As is well known, its current control action is computed by solving a finite horizon optimal control problem on-line. For the receding horizon control, many researchers have tackled the problem of the asymptotical stability. Instead of terminal constraints, a terminal cost may be used with the optimization problem for simplifying its computational demand. As one of key ideas, the receding horizon control with the terminal cost which is a control Lyapunov function of the system is stabilizing control. The application of this method have been done on the Caltech Ducted Fan [2], [3] and on the F-16 Aircraft [4]. In those works, the control Lyapunov function is derived by using quasi-LPV method.

On the other hand, the visual feedback control which involves combination of the robot kinematics, the dynamics and the computer vision systems to control its position and/or orientation should become extremely important when mechanical systems working under dynamical environments. Some recent research efforts which are toward this direction have been nicely collected in [5]. We proposed a Lyapunov based visual feedback control with a planar manipulator [6].

Y. Nakaso and M. Fujita are with the Department of Mechanical and Control Engineering, Tokyo Institute of Technology, Tokyo 152-8552, JAPAN fujita@ctrl.titech.ac.jp

Y. Kawai is with the Department of Electrical Engineering, Ishikawa National College of Technology, Ishikawa 929-0392, JAPAN y_kawai@ishikawa-nct.ac.jp

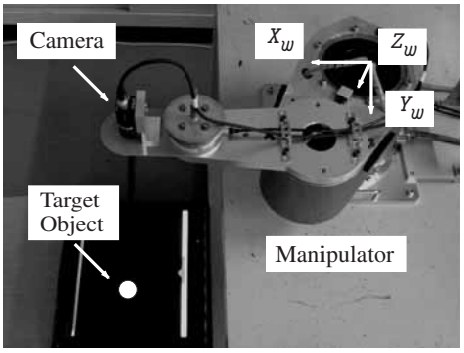

Fig. 1. Two-link direct drive manipulator with a camera

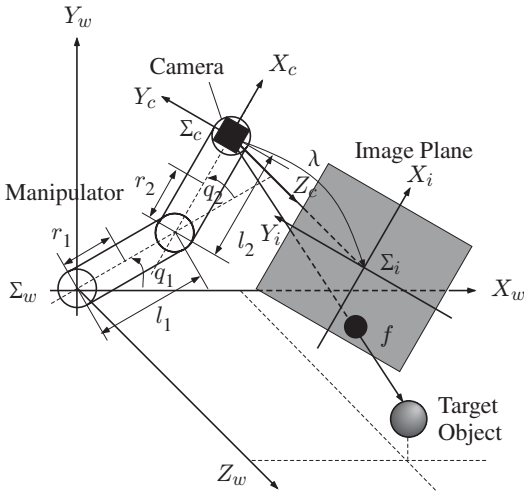

Fig. 2. Schematic diagram of the two-link direct drive manipulator with a camera

Recently, the inverse optimal approach which is an optimal control method considered to avoid the task of solving Hamilton-Jacobi equations is applied to robot motion control or visual feedback system [7], [8]. The optimality with respect to a certain quadratic cost and the stability margins are then provided. This approach was introduced into robust nonlinear control [9]. The effort of [10] is addressed the inverse optimal disturbance attenuation problem from the differential game problem and established the equivalence between the solvability of the problem and the input-to-state stabilizability. These works provide the fact that a stabilizing control on inverse optimality and the quadratic cost are given by the control Lyapunov function. The inverse optimal control for the planar manipulator with a camera has proposed [7], [8].

0-7803-9568-9/05/$20.00 ©2005 IEEE

Although a receding horizon control whose terminal cost is used the control Lyapunov function for that visual feedback system has proposed [11], the inverse optimality was not considered. Furthermore experimental results are not obtained. In this paper, we propose the receding horizon control using a control Lyapunov function as a terminal cost for the visual feedback system. Moreover, the proposed scheme is tested through experiments on the planar manipulator with the eye-in-hand as shown in Fig. 1.

First, we remind the control Lyapunov functions for the visual feedback system. The inverse optimal control scheme is then derived and proves the stability for the system. Next, the receding horizon control scheme for the system using control Lyapunov function is proposed and the stability using this control scheme is guaranteed. Finally, the performance of the receding horizon control scheme is demonstrated through experiments with the two-link direct drive manipulator mounted the camera shown in Fig. 1 and evaluated by comparing with another control schemes.

This paper is organized as follows. The system model and its control Lyapunov function are described in Section II. The inverse optimal controller is designed in Section III. In Section IV, the receding horizon control scheme which utilizes the inverse optimal control scheme is derived. In Section V, the results of the experimental studies are illustrated. Finally, our conclusions are presented in Section VI.

II. Visual Feedback System with Planar Manipulator

A. Description of the System

The manipulator model considered in this paper is the well known Euler-Lagrange system whose inputs are joint torques and whose measurement outputs are joint angles and its angular velocities.

The standard equations describing the dynamics of an n-DOF rigid robot system may be written as

$$M(q)\ddot{q} + C(q,\dot{q})\dot{q} + g(q) = \tau \tag{1}$$

where $M(q) \in \mathbb{R}^{n\times n}$ is the positive definite inertia matrix, and q, $\dot{q}$ and $\ddot{q}$ are the joint angles, angular velocities, and angular accelerations, respectively. The vector $C(q,\dot{q})\dot{q} \in \mathbb{R}^n$ represents the Coriolis and centrifugal force terms, $g(q)$ is the gravity terms and τ is control torques.

We recall the fundamental properties of the inertia matrix of n-link rigid robots [12].

Property 1: The inertia matrix $M(q)$ is symmetric, positive definite, and both $M(q)$ and $M^{-1}(q)$ are uniformly bounded as a function of q.

Property 2: $\dot{M}(q) - 2C(q,\dot{q})$ is skew symmetric.

In the case of $n = 2$, referring to Figs. 1 and 2, terms in the dynamic equation (1) are represented as follows [13] (pp. 164-165).

$$M(q) = \begin{bmatrix} \theta_1 + \theta_2 + 2\theta_3\cos q_2 & \theta_2 + \theta_3\cos q_2 \\ \theta_2 + \theta_3\cos q_2 & \theta_2 \end{bmatrix} \tag{2}$$

$$C(q,\dot{q}) = \begin{bmatrix} -\theta_3\dot{q}_2\sin q_2 & -\theta_3(\dot{q}_1+\dot{q}_2)\sin q_2 \\ \theta_3\dot{q}_1\sin q_2 & 0 \end{bmatrix} \tag{3}$$

$$\theta_1 = m_1 r_1^2 + m_2 l_1^2 + I_1, \tag{4}$$

$$\theta_2 = m_2 r_2^2 + I_2,\ \theta_3 = m_2 l_1 r_2 \tag{5}$$

On the other hand, the camera model should be considered. A CCD camera which is mounted on the end of the manipulator in Fig. 2, is modeled by an ideal perspective transformation. Consider a planar manipulator with the world frame $\Sigma_w = \{X_w\ Y_w\ Z_w\}$ depicted in Fig. 2. It is assumed that the manipulator end-effector evolves in the $X_w - Y_w$ plane of Σ_w. Suppose a camera is mounted on the hand of the manipulator and looking at the object, its optical axis direction is coincident with the Z_w axis direction. The camera has attached a frame $\Sigma_c = \{X_c\ Y_c\ Z_c\}$. A frame $\Sigma_i = \{X_i\ Y_i\}$ is defined in the camera image plane and its origin is the intersection of the optical axis with the image plane. Here it is assumed that axes X_i and Y_i parallel axes X_c and Y_c, respectively, and planes $X_i - Y_i$ and $X_c - Y_c$ are separated by the focal length $\lambda > 0$.

Next the object point P is located at $p_{wo} = [x_{wo}\ y_{wo}\ z_{wo}]^T$ with respect to the frame Σ_w. $f = [f_x\ f_y]^T$ is the image feature parameter vector of P using the pinhole camera model.

Consider a perspective transformation as an ideal pinhole camera model with $\lambda > 0$ being the focal length. The image feature parameter vector f becomes

$$\begin{aligned} f(q) &:= \begin{bmatrix} f_x \\ f_y \end{bmatrix} \\ &= \frac{s\lambda}{z_{wo}} R_{wc}^T(\theta_{wc}(q)) \left(\begin{bmatrix} x_{wo} \\ y_{wo} \end{bmatrix} - \begin{bmatrix} x_{wc}(q) \\ y_{wc}(q) \end{bmatrix} \right) \end{aligned} \tag{6}$$

where $s > 0$ is the scale factor in pixel/m due to the camera sampling and R_{wc} is the rotation matrix [8], [11]. $[x_{wc}\ y_{wc}]^T$ is defined as the position vector of the camera on the $X_w - Y_w$ plane. Then the differential kinematics of the manipulator gives the relationship between the manipulator angular velocities $\dot{q}$ and the velocities of the camera mounted on the end-effector $\dot{p}_{wc}(q)$. The relation can be represented using the manipulator Jacobian $J_b \in \mathbb{R}^{n\times n}$

$$\dot{p}_{wc}(q) := J_b(q)\dot{q}. \tag{7}$$

The image feature dynamics is given by

$$\dot{f} = -\frac{s\lambda}{z_{wo}} R_{wc}^T J_b \dot{q} - R_{wc}^T \dot{R}_{wc} f. \tag{8}$$

Now, we introduce Property 3 that is important for the Lyapunov/passivity based control design.

Property 3: [13] $R_{wc}^T \dot{R}_{wc}$ is skew-symmetric.

The following assumptions will be made throughout the paper.

Assumption 1: There exists a manipulator joint configuration achieving $f = 0$.

Assumption 2: The Jacobian J_b is nonsingular.

Assumption 1 ensures that the control problem is solvable. Assumption 2 is required for technical reasons in the stability analysis.

Here, the rotation matrix R_{wc} and the Jacobian matrix J_b are described as

$$R_{wc} = \begin{bmatrix} \cos(q_1+q_2) & -\sin(q_1+q_2) \\ \sin(q_1+q_2) & \cos(q_1+q_2) \end{bmatrix} \tag{9}$$

$$J_b = \begin{bmatrix} -l_1\sin q_1 - l_2\sin(q_1+q_2) & -l_2\sin(q_1+q_2) \\ l_1\cos q_1 + l_2\cos(q_1+q_2) & l_2\cos(q_1+q_2) \end{bmatrix}. \tag{10}$$

B. Dynamic Visual Feedback System

Consider the visual feedback system model which consists of (1) and (8). The objective of the system is to derive f to the origin. Hence, the camera which is mounted on the end-effector is brought to the position of the target object. To achieve the control objective, the control torque τ is defined as

$$\tau = M(q)\alpha\dot{\eta} + C(q,\dot{q})\alpha\eta + g(q) + u \tag{11}$$

where $\eta := J_b^T R_{wc} f$ and α is a positive definite matrix. The control input vector u is decided by inverse optimal controller or receding horizon controller. Substituting the control torque (11) into (1), the visual feedback system is given as follows.

$$\begin{cases} \dot{\xi} = -M^{-1}(q)C(q,\dot{q})\xi + M^{-1}(q)u \\ \dot{f} = -\dfrac{s\lambda}{z_{wo}}R_{wc}^T J_b \xi \\ \qquad\quad -\left(\dfrac{s\lambda}{z_{wo}}R_{wc}^T J_b \alpha J_b^T R_{wc} + R_{wc}^T \dot{R}_{wc}\right) f \end{cases} \tag{12}$$

where $\xi = \dot{q} - \alpha\eta$. The purpose of this paper is that receding horizon control is applied to the system (12).

C. Energy Function

In the previous work [6] (pp. 73), the guarantee of the asymptotically stability for the equilibrium point of the system is derived from following energy function $V(x)$.

$$V(x) = \frac{1}{2}\xi^T M(q)\xi + \frac{k_p z_{wo}}{2s\lambda} f^T f \tag{13}$$

where $k_p > 0$ is a scalar. The time derivative of V along the solutions to (12) is given by

$$\begin{aligned} \dot{V} &= \xi^T M(q)\dot{\xi} + \frac{1}{2}\xi^T \dot{M}(q)\xi + \frac{k_p z_{wo}}{2s\lambda} f^T \dot{f} \\ &= \xi^T\left(-C(q,\dot{q})\xi + u\right) + \frac{1}{2}\xi^T \dot{M}(q)\xi \\ &\quad + \frac{k_p z_{wo}}{2s\lambda} f^T \left(-\frac{s\lambda}{z_{wo}}R_{wc}^T J_b \xi \right. \\ &\qquad \left. -\frac{s\lambda}{z_{wo}}R_{wc}^T J_b \alpha J_b^T R_{wc} f - R_{wc}^T \dot{R}_{wc} f\right) \\ &= \frac{1}{2}\xi^T\left(\dot{M}(q) - 2C(q,\dot{q})\right)\xi + \xi^T u - k_p f^T R_{wc}^T J_b \xi \\ &\quad - k_p f^T R_{wc}^T J_b \alpha J_b^T R_{wc} f - \frac{k_p z_{wo}}{s\lambda} f^T R_{wc}^T \dot{R}_{wc} f \\ &= \xi^T u - k_p f^T R_{wc}^T J_b \xi - k_p f^T R_{wc}^T J_b \alpha J_b^T R_{wc} f. \end{aligned} \tag{14}$$

where Property 1, 2 and 3 are used. Consider the control input u_p as follows.

$$u_p = -R\xi \tag{15}$$

where R is a positive definite matrix. From (14), the control input u_p derives

$$\begin{aligned} \dot{V} &= -\xi^T R\xi - k_p f^T R_{wc}^T J_b \xi - k_p \alpha f^T R_{wc}^T J_b \alpha J_b^T R_{wc} f \\ &= -x^T Q x \end{aligned} \tag{16}$$

where the state vector x and matrix Q are given by

$$x = \begin{bmatrix} \xi \\ f \end{bmatrix},\ Q = \begin{bmatrix} R & \frac{1}{2}k_p\left(R_{wc}^T J_b\right)^T \\ \frac{1}{2}k_p R_{wc}^T J_b & k_p R_{wc}^T J_b \alpha J_b^T R_{wc} \end{bmatrix}. \tag{17}$$

Thus, R is given by

$$\begin{aligned} R &= \frac{1}{4}k_p\left(R_{wc}^T J_b\right)^T\left(R_{wc}^T J_b \alpha J_b^T R_{wc}\right)^{-1} R_{wc}^T J_b + K \\ &= \frac{1}{4}k_p \alpha^{-1} + K > 0 \end{aligned} \tag{18}$$

where K is a positive definite matrix. Then Q becomes a positive definite matrix, and $\dot{V} < 0$. Therefore the control input u_p is a stabilizing control for the system (12).

III. Inverse Optimal Design of Stabilizing Control

In this section, the inverse optimal control input is derived. An objective function is minimized. Moreover, the stability of the system is guaranteed by the previous energy function.

A. Inverse Optimal Design

Consider an objective function for the system (12) as follows.

$$J_{inv}(u,t) = \lim_{t\to\infty}\left[\int_0^t l(x(\tau),u(\tau))d\tau + V(x(t))\right] \tag{19}$$

The definition for control Lyapunov function $V(x)$ is given by

$$\inf_u\left[\dot{V} + l(x(t),u(t))\right] \le 0 \tag{20}$$

where $l(x(t),u(t))$, which is a positive definite function, will be decided in this section. As a preliminary, the following calculation is considered.

$$\begin{aligned} -4x^T Q x &= -\left(u+2R\xi\right)^T R^{-1}\left(u+2R\xi\right) + u^T R^{-1} u \\ &\quad + 4\xi^T u + 4\xi^T R\xi - 4\xi^T R\xi - 4k_p f^T R_{wc}^T J_b \xi \\ &\quad - 4k_p f^T R_{wc}^T J_b \alpha J_b^T R_{wc} f \\ &= -\left(u+2R\xi\right)^T R^{-1}\left(u+2R\xi\right) + u^T R^{-1} u + 4\dot{V} \\ &= -\left\|u+2R\xi\right\|_{R^{-1}}^2 + u^T R^{-1} u + 4\dot{V} \end{aligned} \tag{21}$$

$$\therefore 4\dot{V} + 4x^T Q x + u^T R^{-1} u = \left\|u+2R\xi\right\|_{R^{-1}}^2 \tag{22}$$

Thus, the inequation (23) is completed.

$$\therefore \inf_u\left[4\dot{V} + 4x^T Q x + u^T R^{-1} u\right] \le 0 \tag{23}$$

For the system (12), consider the objective function $J_{inv}(u,t)$ constructed from control Lyapunov function $V(x)$ and the positive definite function $l(x,u)$ as follows.

$$J_{inv}(u,t) = \lim_{t\to\infty}\Big[\int_0^t l(x(\tau),u(\tau))d\tau + 4V(x(t))\Big] \quad (24)$$

$$l(x,u) = 4x^TQx + u^TR^{-1}u \quad (25)$$

Using (23), (24) and (25) we can calculate the objective function as follows.

$$\begin{aligned} J_{inv}(u,t) &= \lim_{t\to\infty}\Big[\int_0^t l(x(\tau),u(\tau))d\tau + 4V(x(t))\Big] \\ &= \lim_{t\to\infty}\Big[\int_0^t \left(4x^TQx + u^TR^{-1}u\right)d\tau + V(x(t))\Big] \\ &= \lim_{t\to\infty}\Big[\int_0^t \left(\|u+2R\xi\|^2_{R^{-1}} - 4\dot{V}\right)d\tau \\ &\qquad\qquad +4V(x(t))\Big] \\ &= \lim_{t\to\infty}\Big[\int_0^t \|u+2R\xi\|^2_{R^{-1}}\,d\tau + 4V(x(0))\Big] \quad (26) \end{aligned}$$

It is clear that the inverse optimal control law u_{inv} is (27) and minimized objective function J^*_{inv} is (28).

$$u_{inv} = -2R\xi \quad (27)$$

$$J^*_{inv} = 4V(x(0)). \quad (28)$$

Next subsection, it will be shown that the inverse optimal control u_{inv} is also the stabilizing control for the system.

B. Stability Analysis

In previous subsection, it is already shown $V(x)$ is a control Lyapunov function of the system (12). When the control input is to be $u_{inv} = -2R\xi$, derivative of the control Lyapunov function $V(x)$ is given by

$$\begin{aligned} \dot{V} &= -\xi^T 2R\xi - k_p f^T R^T_{wc} J_b \xi - k_p \alpha f^T R^T_{wc} J_b \alpha J_b^T R_{wc} f \\ &= -\begin{bmatrix} \xi \\ f \end{bmatrix}^T \begin{bmatrix} 2R & \frac{1}{2}k_p\left(R^T_{wc}J_b\right)^T \\ \frac{1}{2}k_p R^T_{wc}J_b & k_p R^T_{wc}J_b\alpha J_b^T R_{wc} \end{bmatrix} \begin{bmatrix} \xi \\ f \end{bmatrix} \\ &= -x^TQ'x. \end{aligned} \quad (29)$$

Since Q' is also positive definite matrix, $\dot{V} < 0$. Therefore the equilibrium point of the system is asymptotically stable. The inverse optimal control law (27) is not only minimizing the objective function (24) but also stabilizing the system.

IV. Stabilizing Receding Horizon Control

In this section, stabilizing receding horizon control is derived from the inverse optimal control scheme.

Theorem 1: Consider the objective function for the system (12) as follows.

$$J_{RHC}(u,t) = \int_t^{t+T} l(x(\tau),u(\tau))d\tau + 4V(x(t+T)) \quad (30)$$

Then the receding horizon control with the above objective function stabilizes the system.

Proof: Using (23), (25) and (30) we can calculate the objective function as follows.

$$\begin{aligned} J_{RHC}(u,t) &= \int_t^{t+T} l(x(\tau),u(\tau))d\tau + 4V(x(t+T)) \\ &= \int_t^{t+T} \left(\|u+2R\xi\|^2_{R^{-1}} - 4\dot{V}\right)d\tau \\ &\qquad +4V(x(t+T)) \\ &= \int_t^{t+T} \|u+2R\xi\|^2_{R^{-1}}\,d\tau + 4V(x(t)) \quad (31) \end{aligned}$$

Thus, the objective function is minimized by the control input $u_{RHC} = -2R\xi$ as follows.

$$J^*_{RHC}(t) = J_{RHC}(u_{RHC},t) = 4V(x(t)) \quad (32)$$

Regard the objective function $J^*_{RHC}(t)$ as a Lyapunov function candidate, its time derivative function along the solution of the system (12) is given by

$$\dot{J}^*_{RHC} = 4\dot{V} = -4x^TQ'x. \quad (33)$$

Since Q' is a positive definite matrix, $\dot{J}^*_{RHC} < 0$. Therefore the equilibrium point of the system is asymptotically stable. □

In next section, we apply the receding horizon control to the visual feedback system. It is expected that the performance is improved using the receding horizon control.

V. Experimental Results

In this section, each controller shown in this paper is applied to the two-link robot manipulator with the camera as shown in Fig. 1 and compared their performances. The manipulator is actuated with DC motors and controlled by a digital signal processor (DSP) from dSPACE Inc., which utilizes a powerPC 750 running at 480 MHz. Control programs are written in MATLAB and SIMULINK, and implemented on the DSP using the Real-Time Workshop and dSPACE Software which includes ControlDesk, Real-Time Interface and so on. A XC-HR57 camera is attached at the tip of the manipulator. The video signals are acquired by a frame graver board PicPort-Stereo-H4D and an image processing software HALCON. To solve the real time optimization, the software C/GMRES [15] is utilized. Initial conditions of robot positions and angular velocities are set as follows $q_1(0) = \pi/6$ rad, $q_2(0) = -\pi/6$ rad, and $\dot{q}_1(0) = \dot{q}_2(0) = 0$ rad/s. The target object is positioned at fixed point $f(0) = [-120\ -160]^T$ at first. The control objective is to bring f to the origin. The parameters for the design of each controller set up as follows

$$\frac{s\lambda}{z_{wo}} = \frac{1230}{0.9} = 1367, \quad k_p = 0.13,$$

$$\alpha = \begin{bmatrix} 0.05 & 0 \\ 0 & 0.15 \end{bmatrix}, \quad K = \begin{bmatrix} 0.01 & 0 \\ 0 & 0.01 \end{bmatrix}. \quad (34)$$

The control input with receding horizon control is updating at every 0.02 s. It must be calculated by the receding horizon controller for that period. In this experiment, the

position of the target object is displaced as disturbance to $f = [-50 \ -64]^T$, which are positions from initial position of the camera in an instant around $t = 3$ s. It is expected that the value of the objective function implemented receding horizon controller is to be smallest.

First, performances are compared with three different control schemes, i.e. the receding horizon control, the inverse optimal control and the passivity based control. The closed loop behavior of the system is depicted in Figs. 3 representing responses of ξ, f and u. It is clear that the performance of the closed loop system with a control scheme which consider to minimize the objective function is improved. The performance implemented receding horizon control is not inferior to inverse optimal control one. It is shown that both trajectories are almost same in Figs. 3.

Next, performances of three receding horizon controllers are compared with different horizon lengths. Each response of the system is depicted in Figs. 4 and values of the objective function are given in Table I. Although transient responses are almost same, steady-state responses after $t = 4$ s is different, i.e. the controller in case $T = 1.0$ s is worse than other ones. This means that the longer horizon length does not always bring good performance.

Since it is not clear that the difference of performance between receding horizon controllers in Figs. 4, it should be compared with other directions. The value of the objective function is also compared in Table I. Experiments with three horizon lengths are tested five times for each controller. It is noticed that the value of the objective function is not monotonically increasing in the horizon length. This will be a topic of ongoing interest as this research continues.

VI. Conclusions

The purpose of this paper was to apply the receding horizon control to the dynamic visual feedback system. It was shown that by using a specific terminal cost, the stability of receding horizon scheme was guaranteed. The use of energy function of robot system as a terminal cost, which was derived from the inverse optimal control approach was a key idea. Performances which were derived some control scheme were shown through experiments. It could be seen that the receding horizon control scheme could be applied to robot system and its horizon length played an important role for the performance.

Acknowledgement

The authors would like to thank T. Murao, S. Mimoto and H. Matsuda of Fujita Laboratory, Tokyo Institute of Technology for their time and invaluable help.

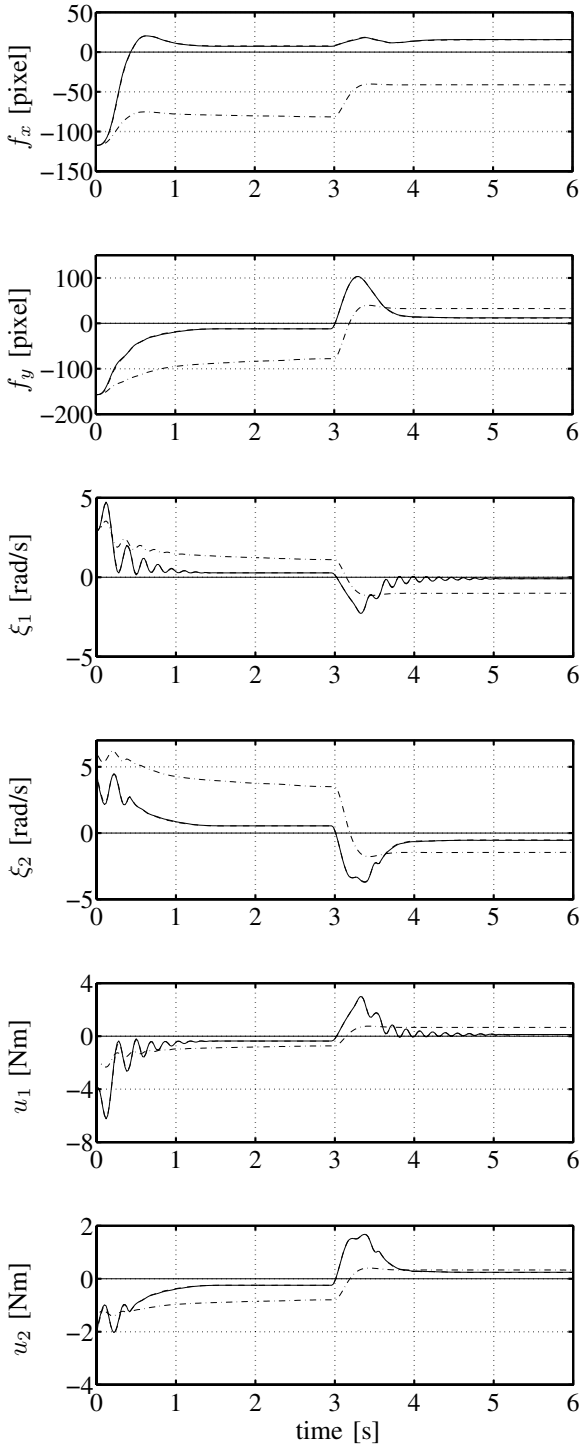

Fig. 3. Experimental comparison with different control schemes (solid: receding horizon control ($T = 0.02$ s), dashed: Inverse optimal control, dot-dashed: passivity based control)

REFERENCES

[1] D. Q. Mayne, J. B. Rawlings, C. V. Rao and P. O. M. Scokaert, "Constrained Model Predictive Control: Stability and Optimality," *Automatica*, vol. 36, no. 7, pp. 789–814, 2000.

[2] J. Yu, A. Jadbabaie, J. Primbs and Y. Huang, "Comparison of Nonlinear Control Design Techniques on a Model of the Caltech Ducted Fan," *Automatica*, vol. 37, no. 12, pp. 1971–1978, 2001.

[3] A. Jadbabaie and J. Hauser, "Control of a Thrust-vectored Flying Wing: a Receding Horizon – LPV Appraoch," *International Journal of Robust and Nonlinear Control*, vol. 12, pp. 869–896, 2002.

[4] R. Bhattacharya, G. J. Balas, M. A. Kaya and A. Packard, "Nonlinear Receding Horizon Control of an F-16 Aircraft," *Journal of Guidance, Control, and Dynamics*, vol. 25, no. 5, pp. 924–931, 2002.

[5] S. Hutchinson, G. D. Hager and P. I. Corke, "A Tutorial on Visual Servo Control," *IEEE Trans. Robotics and Automation*, vol. 12, no. 5, pp. 651–670, 1996.

[6] A, Maruyama and M. Fujita, "Robust Control for Planar Manipulators with Image Feature Parameter Potential," *Advanced Robotics*, vol. 12, no. 1, pp. 67–80, 1998.

[7] A. Maruyama and M. Fujita, "Inverse Optimal H_∞ Disturbance Attenuation of Robotic Manipulators," *Proc. 1999 European Control Conference*, Page Number M806, 1999.

[8] M. Fujita, A. Maruyama, M. Watanabe and H. Kawai, "Inverse Optimal H_∞ Disturbance Attenuation for Planar Manipulators with the Eye-in-Hand System," *Proc. 39th IEEE Conference on Decision and Control*, pp. 3945–3950, 2000.

[9] R. A. Freeman and P. V. Kokotovic, *Robust Nonlinear Control Design*, Birkhauser, 1996.

[10] M. Krstić and Z. Li, "Inverse Optimal Design of Input-to-State Stabilizing Nonlinear Controllers," *IEEE Trans. Automatic Control*, vol. 43, no. 3, pp. 336–350, 1998.

[11] H. Kawai, Y. Kawai, and M. Fujita, "Visual Feedback Control of Planar Manipulators based on Nonlinear Receding Horizon Control Approach," *Proc. 2001 American Control Conference*, pp. 763–768, 2001.

[12] R. Ortega and M. W. Spong, "Adaptive Motion Control of Rigid Robots: a Tutorial," *Automatica*, vol. 25, no. 6, pp. 877–888, 1989.

[13] R. M. Murray, Z. Li and S. S. Sastry, *A Mathematical Introduction to Robotic Manipulation*, CRC Press, 1994.

[14] A. Jadbabaie, J. Yu and J. Hauser, "Unconstrained Receding-Horizon Control of Nonlinear Systems," *IEEE Trans. Automatic Control*, vol. 46, no. 5, pp. 776–783, 2001.

[15] T. Ohtsuka, "A Continuation/GMRES Method for Fast Computation of Nonlinear Receding Horizon Control," *Automatica*, vol. 40, no. 4, pp. 563–574, 2004.

TABLE I

VALUES OF THE OBJECTIVE FUNCTION

Horizon Length	1st	2nd	3rd	4th	5th	average
$T = 0.02$ s	3352	3357	3367	3477	3486	3408
$T = 0.1$ s	3277	3297	3364	3385	3462	3357
$T = 1.0$ s	4097	4158	4204	4211	4252	4184

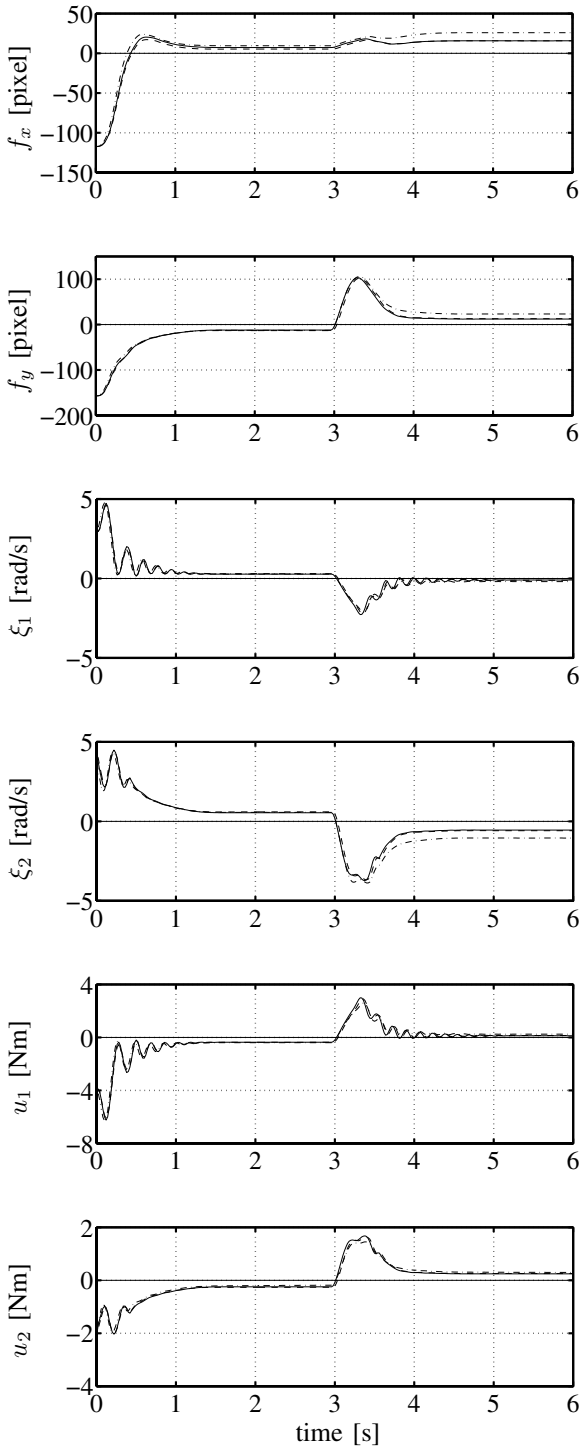

Fig. 4. Experimental comparison with different horizon lengths (solid: $T = 0.02$ s, dashed: $T = 0.1$ s, dot-dashed: $T = 1.0$ s)